

## INFLUENCE OF SOLAR X-RAY FLARES ON THE EARTH-IONOSPHERE WAVEGUIDE

D. Grubor<sup>1</sup>, D. Šulić<sup>2</sup> and V. Žigman<sup>3</sup>

<sup>1</sup>*Faculty of Mining and Geology, Physics Cathedra, University of Belgrade, Serbia and Montenegro*

<sup>2</sup>*Institute of Physics, Belgrade, Serbia and Montenegro*

<sup>3</sup>*Nova Gorica Polytechnic, Nova Gorica, Slovenia*

(Received: October 1, 2005; Accepted: October 18, 2005)

**SUMMARY:** A simultaneous analysis of solar flare X-ray irradiance and VLF signal amplitude on the GQD/22.1 kHz trace was carried out. Solar flare data were taken from GOES 12 satellite listings. The VLF amplitude data were recorded by means of the AbsPAL (Absolute Phase and Amplitude Logger) at the Institute of Physics, Belgrade, Serbia. It was found that solar flare events from class C to class X affect the VLF signal amplitude in various ways and can be classified according to the type of effect produced in the Earth-ionosphere waveguide on the VLF propagation.

**Key words.** Earth – Sun: flares – Sun: x-rays, gamma rays

### 1. INTRODUCTION

It is well known that the X-ray flux emitted from the Sun during flare events can cause additional photoionization of all neutral constituents in the lower ionosphere, including dominant ones as nitrogen and oxygen (Whitten and Poppoff 1965). Furthermore, this source of ionization becomes the major one, exceeding the effects of ionization by all other mechanisms acting in the lower ionosphere. The result of additional ionization is not only the increase of the electron concentration, but also the change of the electron concentration height profile in the ionospheric D region (Thomson and Clilverd 2001). The electron concentration can increase up to two orders of magnitude, from  $10^8 \text{ m}^{-3}$  to  $10^{10} \text{ m}^{-3}$ . The lower edge of the ionosphere, which is the upper edge of the Earth-ionosphere waveguide, descends for several kilometers, from about 74 km to 71-70 km (McRae

and Thomson 2004a). The change of waveguide characteristics affects the propagation parameters of very low frequency signals (VLF). Since the amplitude and phase of the VLF signal are stable under undisturbed solar conditions the appearance of X-ray flare can be detected by the perturbation of the signal phase delay and amplitude (McRae and Thomson 2004b).

There are a number of transmitters all around the world emitting VLF radio waves with very stable phase delay, mainly for the navigation and positioning purposes, or as a time measuring standards. By means of the receiving system situated in Belgrade it is possible to receive, monitor and storage amplitude and phase delay data for six signals on frequencies below 30 kHz. The receiving system is AbsPAL (Absolute Phase and Amplitude Logger) that has been developed by Radio and Space Physics Group of Otago University, New Zealand.

To detect flare effects on the VLF wave propagation medium, we have chosen the signal emitted from Anthorn, UK with code GQD and frequency of 22.1 kHz. There are three reasons for this decision. First, the phase and amplitude of the emitted signal are stable for periods that are long enough to recognize regular diurnal and seasonal patterns in records taken on unperturbed days. Second, the perturbations of phase and amplitude are different as they are due to flares of various characteristics. This fact enables the more detailed classification of flares than the one based only on the peak magnitude of X-ray irradiance. Third, the ray path of the signal crosses two time zones, so the flare affects the propagation medium almost along the entire waveguide. The records taken with time resolution of 60 s were used in the analysis.

## 2. NOTE ON AERONOMY OF THE D REGION

Lower ionosphere, namely the D region, is located approximately between 60 and 95 km above the Earth's surface. The main collision processes in the D region include production and loss of electrons. The production of electrons is due to photoionization processes: a) by UV Lyman- $\alpha$  line, 121.6 nm, b) EUV spectrum between 102.7 nm and 118.8 nm, c) hard X-rays below 0.8 nm, and d) galactic cosmic rays. Each of these mechanisms is the most efficient in some height interval of the D region. In the periods of quiet Sun, the ionization by X-rays is the most efficient at 81-85 km, and also becomes more significant than other mechanisms below 68 km. However, when solar flares appear, the ionization by X-rays becomes the predominant source of electrons in the D region. The main electron loss mechanism is the recombination with positive ions. The condition of quasineutrality in the weakly ionized medium of the D region requires the equality of single ionized particles concentration  $[N_+]$  and electron concentration  $[N_e]$ . Therefore the loss rate  $L$  is proportional to the square of the electron concentration:  $L = \alpha [N_e] [N_+] = \alpha_e [N_e]^2$ , where  $\alpha_e$  is recombination coefficient. At equilibrium the electron production rate  $q$  is equal to loss rate:  $q = \alpha_e [N_e]^2$ . However, electrons are not the only negative particles in the D region the positive ions can be recombined with. There are also negative ions present in the D region, which can recombine with positive ions. If the concentration of negative ions is  $[N_-]$ , than equilibrium is achieved with  $q = \alpha_e [N_e]^2 + \alpha_i [N_e] [N_-]$ , where  $\alpha_i$  is the recombination coefficient of negative ions with positive ions. Both processes lead to "effective recombination" decreasing ionization level in the D region (Hargreaves 1992). Nevertheless, only the loss of electrons will be of our concern, because the propagation of radio waves in ionized medium is carried out by interaction with electrons.

## 3. THE PROPAGATION OF VLF RADIO WAVES

The characteristics of the lower boundary of the Earth-ionosphere waveguide are determined by electrical conductivity of soil and water surface along the grand circle of the ray path. The upper boundary of the Earth-ionosphere waveguide changes its characteristics with diurnal and seasonal variations of lower ionosphere. These changes are predictable, so may be considered as regular. The unpredictable changes occur when abrupt change of electron concentration in the D region takes place and therefore the reflection coefficient changes at locations containing the wave reflection points. One of the causes that affect the waveguide upper boundary is the ionization by a solar X-ray flare. In this paper we will deal with *unpredictable* changes of waveguide characteristics.

The change of waveguide upper boundary, caused by a solar flare X-ray burst, can be manifested in two main ways: a) sharpness of the boundary of the D region due to an increase of electron concentration simultaneously with a descent of the boundary and b) increase of electron content in the entire D region, without sharpness of the boundary. In case a) the reflection of "mirror" type occurs, and the propagation calculations can be carried out in the same way as if the boundary surface had metal characteristics. The dissipation of wave energy is negligible, even smaller than in the unperturbed propagation conditions. The effect of such disturbance of the D region is a rise of the received VLF signal amplitude to the maximum, than decreasing to unperturbed value, following the magnitude of the solar X-ray irradiance. In case b) the wave penetrates into the D region, up to the altitude at which the wave frequency matches the plasma frequency of the medium and where the reflection takes place. Along the ray path inside the D region, so called "deviative" absorption from point to point is present and wave energy is dissipated at each step (Budden 1961). The result is a drop of the received VLF signal amplitude to the minimum followed by a rise to unperturbed value, corresponding to the end of the solar flare X-ray burst. In both cases a) and b) the phase delay follows the variation of the amplitude, but the changes are not necessarily of the same sign. However, an intermediate regime of propagation is possible too. Our goal is to find out the flare characteristics determining the conditions under which the propagation mode changes from case a) to case b).

The amplitude and the phase delay along the ray path from the transmitter to the receiver undergo oscillations of magnitude in accordance with changes of the reflection coefficient at reflection points, both on the lower and on the upper boundary of the waveguide. The "full wave" analysis was developed (Ferguson 1995) to calculate propagation parameters of the ray path in a general case. The complete treatment of wave propagation parameters can only be performed using appropriate computer pro-

**Table 1.** Parameters of the lower ionosphere as propagation medium for 22.1 kHz waves;  $N_e$  is the electron concentration,  $\nu$  is the electron-neutral collision frequency,  $\omega_N$  is the plasma frequency and  $\omega = 2\pi \cdot 22.1 \text{ rads}^{-1}$  is the wave frequency.

height [km]	$N_e [\text{m}^{-3}]$	$\nu [\text{s}^{-1}]$	$\omega_N^2 [\text{s}^{-1}]^2$	$Z=\nu/\omega$	$\omega_N^2/\nu$
89.3	$2.14 \cdot 10^9$	$2.77 \cdot 10^5$	6.81E+12	1.99E+00	2.46E+07
74.1	$2.18 \cdot 10^8$	$2.72 \cdot 10^6$	6.92E+11	1.96E+01	2.55E+05
43.4	$2.18 \cdot 10^6$	$2.72 \cdot 10^8$	6.92E+09	1.96E+03	2.55E+01

**Table 2.** Propagation path parameters for the trace Anthorn-Belgrade.

$\phi$	$\lambda$	$\theta$	dip	B [T]	$\sigma$ [S]	$\varepsilon/\varepsilon_0$	$\beta [\text{km}^{-1}]$	$h' [\text{km}]$
54.37°	3.17°	121.77 °	68.86°	$4.705 \cdot 10^5$	4	81.0	0.30	74.0

grams. Such program was produced by Space and Naval Warfare System Center, San Diego (Ferguson 1998) and named Long-Wavelength Propagation Capability (LWPCv21). We have used this program for calculations of the ray path and propagation parameters of GQD/22.1 kHz. In Fig. 1, the variation of the signal amplitude and phase delay along the great circle path is shown.

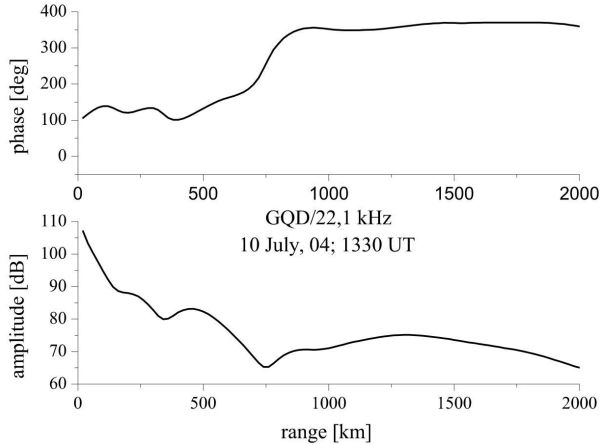


**Fig. 1.** The variation of the GQD/22.1 kHz signal amplitude and phase delay along the range of 2000 km on the great circle path, from Anthorn ( $54^\circ 53' N$ ,  $3^\circ 17' W$ ) to Belgrade ( $44^\circ 51' N$ ,  $20^\circ 23' E$ ) on the day without solar X-ray flares. Note the minimum mode of the amplitude at reflection point 750 km away from transmitter.

To obtain amplitude and phase delay variation as shown in Fig. 1, one has to use input parameters shown in Table 1 and Table 2.

The meaning of symbols in Table 2, is as follows: at the location of Anthorn transmitter  $\phi$  is the latitude North,  $\lambda$  is the longitude West,  $\theta$  is the azimuth, dip is the inclination angle of the magnetic field, B is the strength of the magnetic field,  $\sigma$  is the ground conductivity,  $\varepsilon/\varepsilon_0$  is the relative dielectric constant of the ground, the exponential increase in conductivity with height is specified by the slope  $\beta$  and  $h'$  is the reference height.

The calculated amplitude value of 65 dB, obtained by LWPCv21 program, is in good agreement with the measured value of 63 dB, at 13:30 UT on 10 July, 2004, at Belgrade station. The calculated value for phase delay ( $359^\circ$ ) does not match with the measured value ( $337^\circ$ ) so well, but the difference is still acceptable. Diurnal variation of amplitude and phase for 22.1 kHz are plotted in Fig. 2.

#### 4. THE SIMULTANEOUS MONITORING OF VLF WAVE AMPLITUDE AND X-RAY FLUX

The typical example of a signal amplitude and phase delay diurnal change observed on a very quiet summer day, 10 July, 2004 is shown in Fig. 2. From data recorded by GOES 12 satellite it can be seen that the X-ray irradiance  $I_X$ , did not exceed magnitude of  $10^{-6} \text{ W/m}^2$ , namely, no significant flare events occurred.

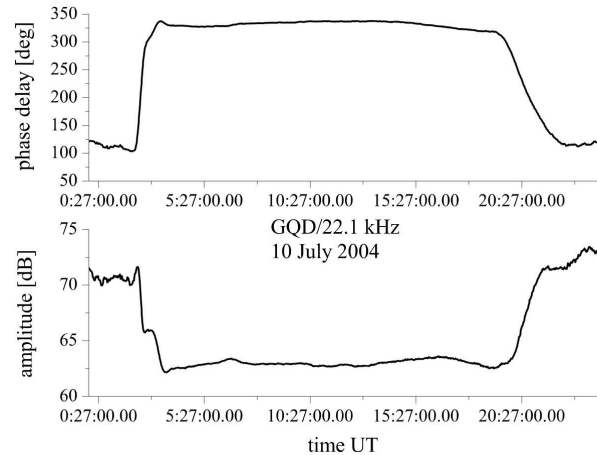


**Fig. 2.** Diurnal variation of the GQD signals amplitude and phase, during day without significant flares, 10 July, 2004. Universal Time is used. The amplitude is measured in dB over  $1 \mu\text{V/m}$ .

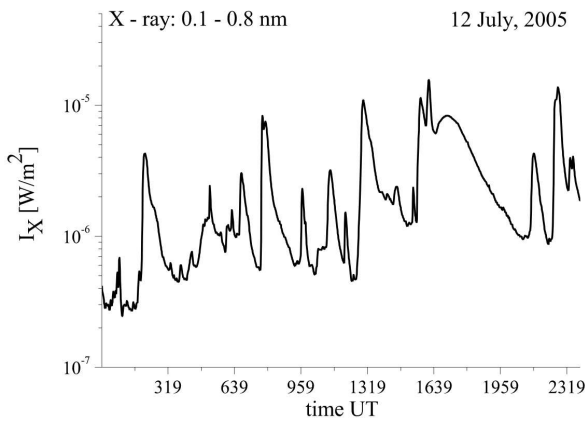


**Fig. 3.** Diurnal variation of the X-ray irradiance, on a very disturbed day, 12 July, 2005. Up to 15 significant flares, with  $I_X$  peaks exceeding  $10^{-6}$  W/m<sup>2</sup>, can be seen.

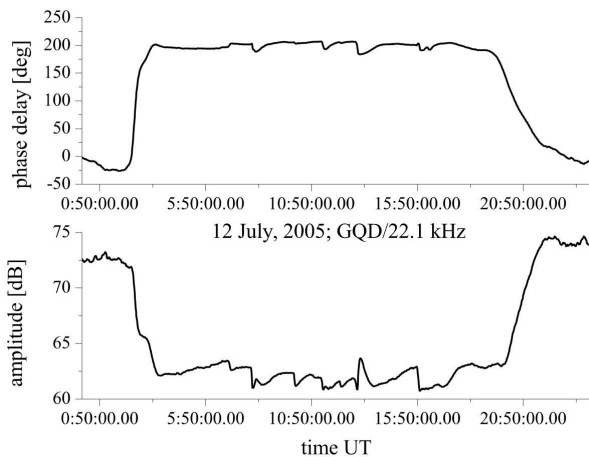


**Fig. 4.** Diurnal variation of the GQD signal amplitude and phase, on a very disturbed day, 12 July, 2005.

According to GOES 12 data listings, the series of C-class ( $10^{-5} > I_X \geq 10^{-6}$  W/m<sup>2</sup>) and M-class ( $10^{-4} > I_X \geq 10^{-5}$  W/m<sup>2</sup>) flares, appeared on 12 July, 2005, which can be considered as a very disturbed day. The corresponding diurnal distribution of the X-ray irradiance is shown in Fig. 3. Each of these flares caused a disturbance of the signal amplitude and phase delay as evident from plots given in Fig. 4. However, the effects of flares that appeared before the sunrise and after the sunset are not apparent, because the day/night changes of propagation medium are more severe than influences of even the strongest flares. The detailed inspection of Fig. 4 shows a presence of three main types of flare effects on signal amplitudes: a decrease, decrease with oscillation, sudden drop followed by an increase up to a peak value. These features can be better recognized as time-isolated events, at series of transcen-

dent events. Typical examples are given in Figs. 5 - 10. On each plot, the simultaneous change of signal amplitude and X-ray irradiance during the time interval enclosing the flare event are presented. Time axes are given in the Universal Time. The local time at the receiver is given by UT + 1h 22' and at the Anthorn-Belgrade trace midpoint local time is UT + 0h 37', so the major part of the trace Anthorn-Belgrade is sunlit around the UT noon. Therefore, all flares occurring around the UT noon are expected to disturb the wave amplitude and phase delay, (the zenith angle for the trace midpoint is close to zero). Flares appearing at dusk or dawn (zenith angle for the trace midpoint is close to  $\pm 90^\circ$ ) are also efficient, if strong enough.

## 5. OBSERVATIONS

Solar flares class C1 - C3 (with peaks  $I_X$ :  $10^{-6}$  -  $3.9 \cdot 10^{-6}$  W/m<sup>2</sup>) cause predominately "pure negative changes", namely a rapid decrease of amplitude to a minimum and much slower recovery to its value preceding the flare. The minimum amplitude value is time delayed with respect to the X-ray peak irradiance. The delay time ( $\Delta t$ ) is few minutes, and it is due to the "sluggishness" of the ionosphere (Appleton 1953) in reaching the peak electron concentration. Sluggishness of the ionosphere is caused by recombination processes, as mentioned in Section 2. The difference between the extreme amplitude value and the value of amplitude at the moment corresponding to the extreme value, but on the nearest undisturbed day ( $\Delta A$ ), is up to 2 dB. The typical example of such flare effect is given in Fig. 5. Amplitude difference is  $\Delta A \approx -1.2$  dB and delay time is  $\Delta t = 4$  min.

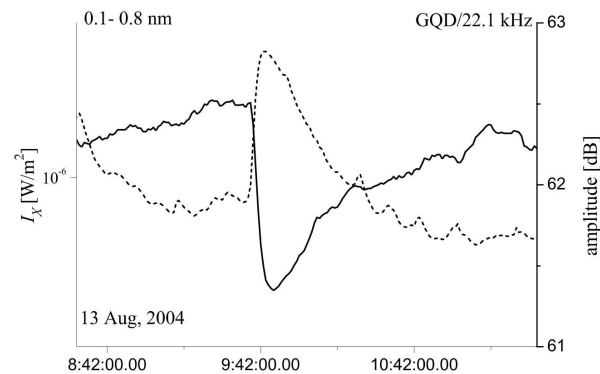


**Fig. 5.** Solar flare event (dashed line) with a peak X-ray irradiance at 09:43 UT on 13 August, 2004 and the corresponding disturbance of VLF signal amplitude (solid line).

The X-ray irradiance with a peak greater than  $I_X \approx 4 \cdot 10^{-6}$  W/m<sup>2</sup>, causes a more complicated effect. As  $I_X$  increases, the amplitude value decreases, but the decrease terminates before the X-ray irradi-

ance reaches the peak value. After the moment of the first minimum, the amplitude oscillates passing through a small peak delayed a few minutes with respect to the peak of X-ray irradiance and through the second minimum. After that, the amplitude slowly recovers to its value before the flare. The example of this flare effect is given in Fig. 6. The solar flare is class C8.4, (peak  $I_X = 8.44 \cdot 10^{-6} \text{ W/m}^2$ ). The amplitude difference at the moment of the first maximum is  $\Delta A \approx -3 \text{ dB}$  and the delay time between the X-ray peak and the amplitude peak is  $\Delta t = 3 \text{ min}$ .

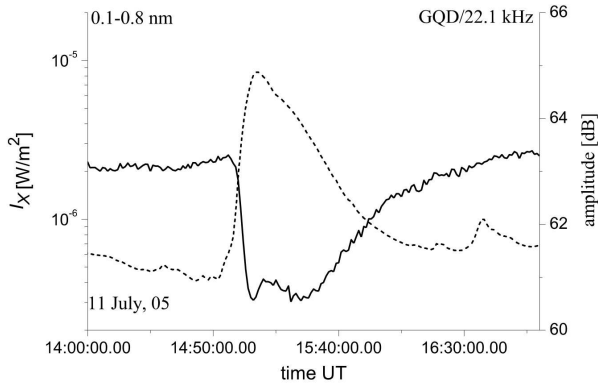


**Fig. 6.** Solar flare event (dashed line) with peak X-ray irradiance at 15:07 UT on 11 July, 2005 and corresponding disturbance of VLF signal amplitude (solid line). The characteristic events took place at time: 15:06 UT (first minimum), 15:10 UT (small amplitude peak), and 15:26 UT (second minimum).

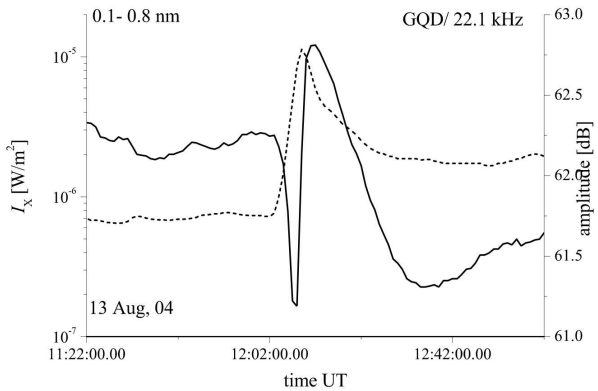


**Fig. 7.** Solar flare event (dashed line) with peak X-ray irradiance at 12:09 UT on 13 August, 2004 and corresponding disturbance of VLF signal amplitude (solid line). The characteristic events took place at time: 12:08 UT (first minimum), 12:12 UT (amplitude peak), and 12:35 UT (second minimum).

If solar flares of M1 class (with peaks  $I_X$  around  $10^{-5} \text{ W/m}^2$ ) occur, the amplitude peak be-

tween the first and the second minima arises above the level of the undisturbed amplitude value, as shown in Fig. 7. The amplitude difference at the moment of the first maximum is  $\Delta A_1 \approx -1.1 \text{ dB}$ , at the moment of the peak amplitude  $\Delta A_1 \approx 0.6 \text{ dB}$  and the delay time between X-ray peak and the amplitude peak is  $\Delta t = 3 \text{ min}$ .

Solar flares of class M2 or higher, increase amplitude peaks by several dB above the level of the undisturbed amplitude. The effect is shown in Fig. 8, for two similar disturbances caused by two solar flares of class M5.4 and M3.0. The amplitude peak becomes the dominant feature in the amplitude variation during the solar flare. Nevertheless, the peak is followed by the decrease, below the level of the undisturbed amplitude. The M5.4 class flare causes the amplitude difference at the moment of peak amplitude  $\Delta A \approx 4.4 \text{ dB}$  and delay time from X-ray peak to the amplitude peak is  $\Delta t = 4 \text{ min}$ . The M3.0 class flare causes an amplitude difference  $\Delta A \approx 3.2 \text{ dB}$  and delay time  $\Delta t = 1 \text{ min}$ .

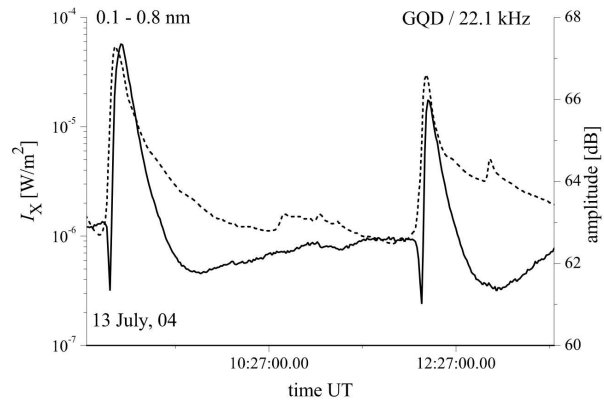


**Fig. 8.** Two solar flare events (dashed line) with peak X-ray irradiance at 08:48 UT and 12:08 UT respectively, on 13 July, 2004 and corresponding disturbances of VLF signal amplitude (solid line).

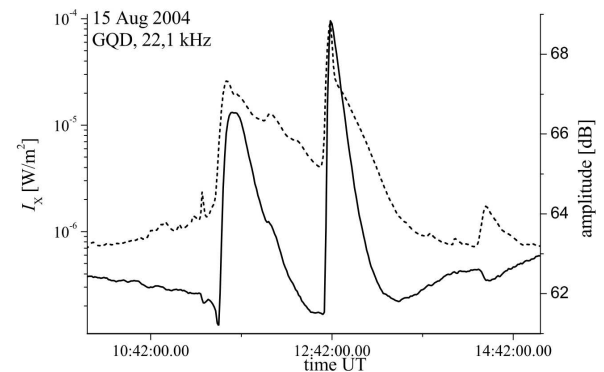


**Fig. 9.** Two successive solar flare events (dashed line) with peak X-ray irradiance at 11:32 and 12:41 UT respectively, on 15 August, 2004 and corresponding disturbances of VLF signal amplitude (solid line).

For even greater flare events, M5 - M9, the first amplitude minimum becomes less expressed until it disappears, as it can be seen in Fig. 9, for the second of two close disturbances. The M2.6 class flare cause the amplitude difference at the moment of peak amplitude  $\Delta A \approx 4.2$  dB and delay time from X-ray peak to the amplitude peak is  $\Delta t = 4$  min. The M9.4 class flare causes an amplitude difference  $\Delta A \approx 6.6$  dB and delay time  $\Delta t < 1$  min.

The X class flare with peak irradiance  $I_X = 1.69 \cdot 10^{-4}$  W/m<sup>2</sup>, at 18:24 UT on 15 July, 2004 caused pure negative effect on VLF signal amplitude. The amplitude minimum appeared with delay time  $\Delta t = 4$  min and amplitude difference is about 3.5 dB. The slow recovery of the amplitude merges with its regular enhancement at dusk hours.

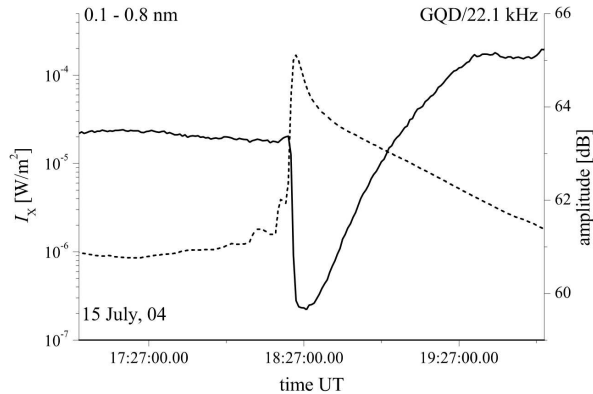


**Fig. 10.** Solar flare event (dashed line) with peak X-ray irradiance at 18:24 UT on 15 July, 2004 and corresponding disturbance of VLF signal amplitude (solid line).

## 6. DISCUSSION AND CONCLUSIONS

The qualitative explanation of the features presented in Figs. 5-10 is given as follows. The small decreases of the VLF signal amplitude, caused by C class flares (as the one shown in Fig. 5) are due to the deviative absorption of wave energy in the D region. Namely, the VLF wave penetrates into the D region in which the ionization by X-ray burst slightly increases the electron concentration. The reflection points from the upper boundary of the Earth-ionosphere waveguide are situated deeper in the region, so the ray path through the ionized medium with a greater electron concentration is longer than during the undisturbed conditions.

As the X-ray irradiance increases, two phenomena take place, one is the increase of the electron concentration and the other is electron concentration redistribution with height. The upper boundary of the Earth-ionosphere waveguide descends to the lower altitude and a reflection of VLF waves occurs at sharp boundary, without penetration into region, (the "mirror" type reflection). The transition of the reflection based on deviative absorption to the

mirror reflection, takes few minutes. Actually, it occurs in the time necessary for X-ray irradiance to reach a certain value, which is from  $5 \cdot 10^{-6}$  to  $10^{-5}$  W/m<sup>2</sup>. Therefore, the C5 to M1 class flares cause the drop of VLF signal amplitude to the minimum in first few minutes (due to deviative absorption), followed by the rise of the amplitude to a small peak (due to mirror reflection), delayed few minutes after the peak X-ray irradiance. Decreasing of the X-ray irradiance causes ascending and diminishing of the sharp boundary, allowing the penetration of the wave deeper in the D region. The deviative absorption occurs again and the value of amplitude decreases to the second minimum. This effect is presented in Fig. 6.

The variation of amplitude during the flare as described above, generally holds for greater M class flares and for X class flares. The greater the X-ray peak irradiance, the higher the amplitude peak above the level of the regular diurnal value. The transient case is shown in Fig. 7, and the case with two outstanding peaks is shown in Fig. 8. Finally, if the peak X-ray irradiance approaches  $10^{-4}$  W/m<sup>2</sup>, the amplitude change is pure positive, as shown by second disturbance in Fig. 9.

However, if the X class solar flare occurs at the high solar zenith angle with respect to the midpoint of the VLF wave trace (dusk or down hours), the effect on the VLF signal amplitude will be negative, as shown in Fig. 10. Namely, the electron concentration even if increased by X-ray ionization, is still insufficient to form the sharp upper boundary of the Earth-ionosphere waveguide, at low altitude. Therefore, the deviative absorption of VLF wave takes place, and the effect is similar as the one shown in Fig. 5.

## REFERENCES

- Appleton, E. V.: 1953, *Atmospheric and Terrestrial Physics*, **3**, 282.
- Budden, K. G.: 1961, *The Waveguide Mode Theory of Wave Propagation*, Logos Press, London.
- Ferguson, J. A.: 1995, *Radio Science*, **30** (3), 775.
- Ferguson, J. A.: 1998, *Computer Programs for Assessment of Long-Wavelength Radio Communications*, Version 2.0, Space and Naval Warfare Systems Center, San Diego CA.
- Hargreaves, J. K.: 1992, *The solar-terrestrial environment*, Cambridge University Press.
- McRae, W. M., Thomson, N. R.: 2004a, *Journal of Atmospheric and Solar-Terrestrial Physics*, **66**, 77.
- McRae, W. M., Thomson, N. R.: 2004b, *Journal of Atmospheric and Solar-Terrestrial Physics*, **62**, 609.
- Thomson, N. R., Clilverd, M. A.: 2001, *Journal of Atmospheric and Solar-Terrestrial Physics*, **63**, 1729.
- Whitten R. C., Poppoff I. G.: 1965, *Physics of the Lower Ionosphere*, Prentice-Hall, Inc. Englewood Cliffs, N. J.

**УТИЦАЈ Х-ЗРАЧЕЊА ТОКОМ СОЛАРНИХ ФЛЕРОВА  
НА ТАЛАСОВОД ЗЕМЉА – ЈОНОСФЕРА****D. Grubor<sup>1</sup>, D. Šulić<sup>2</sup> and V. Žigman<sup>3</sup>**<sup>1</sup>*Faculty of Mining and Geology, Physics Cathedra, University of Belgrade, Serbia and Montenegro*<sup>2</sup>*Institute of Physics, Belgrade, Serbia and Montenegro*<sup>3</sup>*Nova Gorica Polytechnic, Nova Gorica, Slovenia*

*Оригинални научни рад*  
UDK 52-853 : 523.985.3-73

Анализиран је интензитет Х-зрачења током соларног флера и амплитуде сигнала врло ниских фреквенција (Very Low Frequency) на траси GQD/22.1 kHz, за исте временске интервале. Подаци о соларним флеровима узети су из листа регистрација сателитског система GOES 12. Подаци о амплитудама VLF сигнала добијени су путем система за пријем и бележење апсолутне вредности фазе и ампли-

туде, (AbsPal), који је смештен у Институту за физику у Београду. Установљено је да соларни флерови, од оних класе С до оних класе Х, утичу на амплитуду VLF сигнала на различите начине и могу да се класификују у односу на тип ефекта који изазивају при простирању VLF таласа, таласоводом Земља-јоносфера.